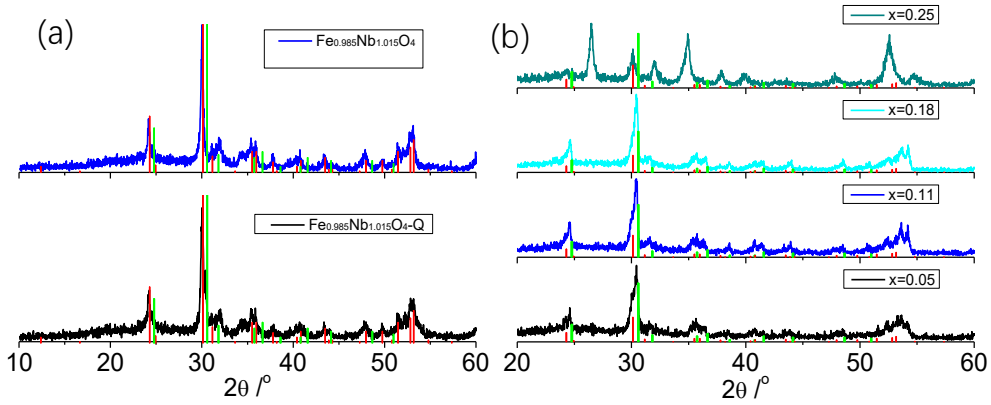

Figure S1 XRD of the $Fe_{0.985}Nb_{1.015}O_4$ with and without quenching (a) and the $Ti_{2x}(Fe_{0.985}Nb_{1.015})_{1-x}O_4$ powders (b) after the reduction at 700 °C in 5% H_2. The vertical bars represent the powder diffraction (PDF) of orthorhombic $FeNbO_4$ (green) and $FeNb_2O_6$ (red). The rutile $Ti_{0.5}(Fe_{0.985}Nb_{1.015})_{0.75}O_4$ decomposes to $FeNb_2O_6$ after the reduction process while the α-PbO_2 type oxides with TiO_2 are stable.

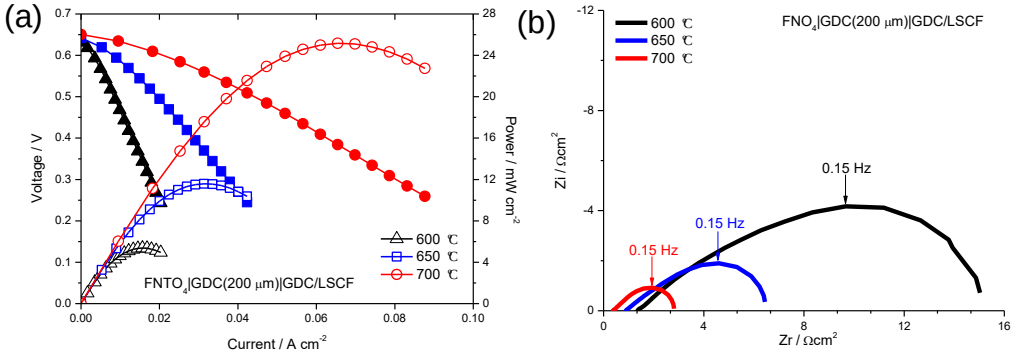

Figure S2 I-V and I-P curve of the cell (a) at 600 °C, 650 °C and 700 °C and the corresponding Nyquist plots of electrochemical impedance spectra (b) at OCV.

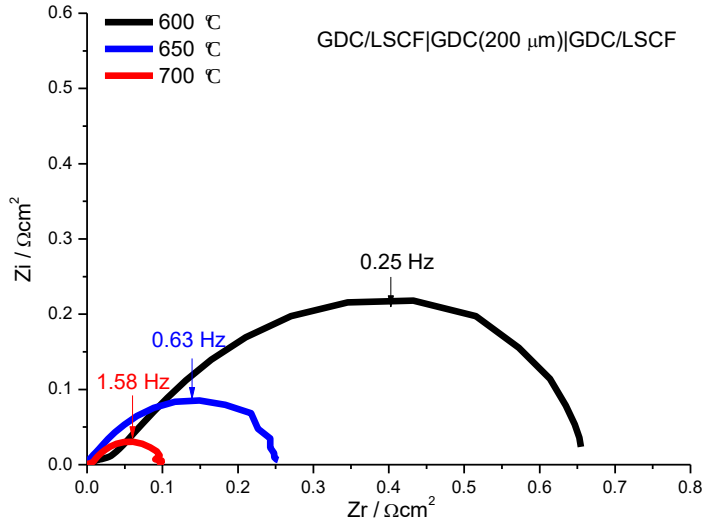

Figure S3 Nyquist plots of electrochemical impedance spectra for the LSCF cathode for the symmetrical electrode at 600 °C, 650 °C and 700 °C (the ohmic resistance is subtracted).

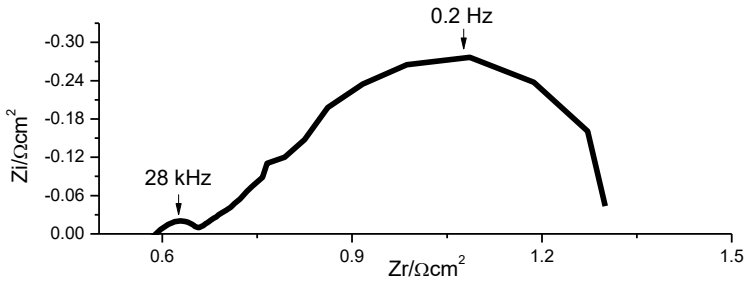

Figure S4 Electrochemical impedance spectra of the cell with TFN-36 anode under LPG fuel at 700 °C.

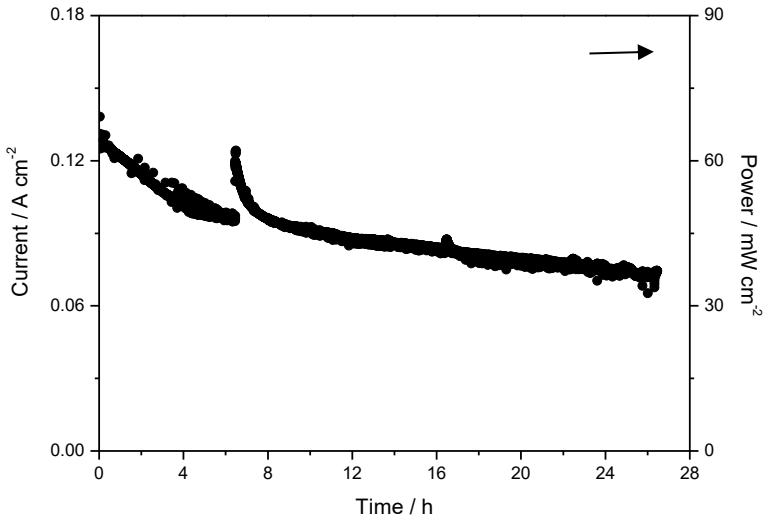

Figure S5 Evolution of the current density and the power of the cell with TFN-36 anode under LPG gas at 0.5 V.